Approximate universality at a first-order transition-the three-state Potts model in (3+1) dimensions

1994 J. Phys. A: Math. Gen. 27 5789

(http://iopscience.iop.org/0305-4470/27/17/013)

J. Phys. A: Math. Gen. 27 (1994) 5789–5800. Printed in the UK

Approximate universality at a first-order transition—the three-state Potts model in (3+1) dimensions

Zheng Weihong†, C J Hamer‡ and J Oitmaa§

School of Physics, The University of New South Wales, Sydney, NSW 2052, Australia

Received 2 June 1994

Abstract. Both 'high-' and 'low-temperature' perturbation series are used to locate and characterize the first-order transition in the three-state Potts model in (3+1) dimensions on the simple-cubic, body-centred cubic and face-centred cubic lattices. Estimates are presented for the vacuum energy, 'latent heat', magnetization, susceptibility and mass gap at the transition. The results show a remarkable degree of universality between the different lattices, and a 'law of corresponding states' is followed very closely.

1. Introduction

The model discussed in this work is the three-state Potts model in (3+1) dimensions, the quantum Hamiltonian equivalent of the normal Euclidean Potts model in four dimensions. As part of a programme of series investigations, we have carried out both 'high-' and 'low-temperature' expansions for the ground-state energy, the mass gaps, the susceptibility and the magnetization for the model. These are analysed in order to study the nature of the phase transition.

The order of the phase transition for this model is not in doubt. Aharony and Pytte (1981) performed a renormalization-group analysis of the Potts model in (and near) four dimensions, and showed that the transition is first-order for the p-state model if $p > 2$. Our results provide very clear confirmation of this prediction. Having both high- and low-temperature expansions at hand, one can extrapolate towards the transition from both sides simultaneously, and thus deduce with high accuracy the location of the transition point, and the discontinuities that occur there. These calculations are performed for three different lattices, namely the simple cubic (SC), the body-centred cubic (BCC) and the face-centred cubic (FCC).

The most interesting feature of the results is a remarkable degree of universality between the results for the different lattices. The discontinuity in the magnetization at the transition point, for instance, is the same for all three lattices, to within an accuracy of a couple of per-cent. When plotted against the reduced 'temperature' variable, the magnetizations for all three lattices fall on a universal curve; in other words, they obey a 'law of corresponding states'. Other observables such as the mass gaps and susceptibility display a similar behaviour, at a somewhat lesser level of accuracy. The same universal behaviour has also been observed in the (2+1)-dimensional version of the model (Hamer *et al* 1992).

† E-mail address: w.zheng@unsw.edu.au
‡ E-mail address: c.hamer@unsw.edu.au
§ E-mail address: otja@newt.phys.unsw.edu.au

0305-4470/94/175789+12$19.50

Universality is normally expected to be a characteristic of second-order, rather than first-order transitions. It is understood via renormalization-group theory on the basis that the correlation length near the critical point becomes very large compared to the lattice spacing, so that microscopic details of the system become unimportant. As we argued previously (Hamer *et al* 1992), the same argument can apply at a first-order transition, provided it is only 'weakly' first-order, i.e. the correlation length is sufficiently large. One must presume that in this case the universality is only approximate. The results are nevertheless very striking, in the present case.

2. Method

The 'high-temperature' (HT) form of the Hamiltonian for this model is

$$H = -2\sum_i \cos\left(\frac{2\pi}{3}L_i\right) - \lambda \sum_{\langle ij\rangle} \left(R_i^+ R_j^- + R_i^- R_j^+\right) \tag{2.1}$$

where i labels the sites on a three-dimensional spatial lattice, $\langle ij\rangle$ denotes nearest-neighbour pairs of sites, and λ is the coupling (corresponding to the inverse temperature in the Euclidean formulation). If λ is very large, then the model can be described by a 'low-temperature' (LT) form of the Hamiltonian

$$H' = -2\sum_{\langle ij\rangle} \cos\left[\tfrac{2}{3}\pi(L_i - L_j)\right] - \lambda' \sum_i (R_i^+ + R_i^-) \tag{2.2}$$

where in both cases L_i, $R_i^{\pm}$ are operators at each site which in a basis of eigenstates of L_i obey the rules:

$$L_i|l_i\rangle = l_i|l_i\rangle \qquad l_i = 0,\ 1,\ 2 \tag{2.3}$$

and

$$R_i^{\pm}|l_i\rangle = |(l_i \pm 1) \bmod 3\rangle \tag{2.4}$$

so that $R_i^{\pm}$ are raising and lowering operators for the spin l_i, modulo 3. The two versions of the Hamiltonian are related by

$$H(\lambda) = \frac{1}{\lambda'} H'(\lambda') \qquad \lambda = 1/\lambda' . \tag{2.5}$$

Using the linked-cluster series-expansion method (Nickel 1980, He *et al* 1990, Hamer *et al* 1992), both 'high-temperature' series in λ and 'low-temperature' series in λ' have been calculated for the ground-state energy, the mass gap, the magnetization, and the susceptibility of the model for SC, BCC and FCC lattices. In these calculations, the first term in (2.1) and (2.2) is taken as the unperturbed Hamiltonian, diagonal in the basis of eigenvectors of L_i, while the second term then acts as a perturbation, which 'flips' the spin at site i for the low-temperature expansion, or on neighbouring pairs of sites $\langle ij\rangle$ for the high-temperature expansion.

To calculate the susceptibility in the high-temperature expansion, we need to add a magnetic term

$$H_M = h\sum_i (R_i^+ + R_i^-)/2 \tag{2.6}$$

to the Hamiltonian (2.1), and then the susceptibility is defined as

$$\chi = -\frac{1}{N}\frac{\partial^2 E_0(h,\lambda)}{\partial^2 h}\bigg|_{h=0} \tag{2.7}$$

where N is the number of lattice sites.

For the low-temperature expansion, the magnetic field term to be added to the Hamiltonian (2.2) is taken as

$$H'_{\mathrm{M}} = h' \sum_{i} \cos\left(\tfrac{2}{3}\pi L_i\right) \tag{2.8}$$

and the spontaneous magnetization and susceptibility are defined as:

$$M'_0 = \frac{1}{N}\frac{\partial E'_0(h',\lambda')}{\partial h'}\bigg|_{h'=0} \qquad \chi' = -\frac{1}{N}\frac{\partial^2 E'_0(h',\lambda')}{\partial^2 h'}\bigg|_{h'=0}. \tag{2.9}$$

There are two sectors of excited states in the model, symmetric and antisymmetric, respectively, under a spin-parity transformation. The lowest excited state in each sector is a single site excitation, in both the HT and LT phases. In the high-temperature series expansion the two states have the same eigenvalues F^{S} and F^{A}, but in the low-temperature expansion the two states differ, except in the limit of $\lambda' = 0$.

The relations between the high- and low-temperature observables are, respectively,

$$E_0(\lambda) = \frac{1}{\lambda'}E'_0(\lambda') \tag{2.10}$$

$$\chi(\lambda) = \lambda'\chi'(\lambda') \tag{2.11}$$

$$F^{\mathrm{S,A}}(\lambda) = \frac{1}{\lambda'}F'^{\mathrm{S,A}}(\lambda') \tag{2.12}$$

with $\lambda = 1/\lambda'$.

Series have been calculated for the ground-state energy per site E_0/N, the magnetization M_0, the susceptibility χ, and the symmetric and antisymmetric lowest-lying excited state eigenvalues F^{S}, F^{A} on the SC, BCC and FCC lattices. The perturbation series for each quantity was calculated using the linked-cluster expansion method, reviewed by He *et al* (1990). For the calculation of the ground-state energy, a list of all connected clusters up to a certain order are needed, while for the calculation of the mass gap, both connected and disconnected clusters are needed. Table 1 gives the number of clusters generated for each lattice. Tables 2–4 give the resulting series coefficients in the 'high-' and 'low-temperature' regimes.

Table 1. The number of clusters generated for each lattice. Here nv is the number of sites (vertices), and nb is the number of bonds (edges).

		Ground-state energy		Mass gap	
Lattice	Expansion	Order	No of clusters	Order	No of clusters
SC	HT	$nb = 10$	824	$nb = 10$	2662
SC	LT	$nv = 10$	1050	$nv = 9$	717
BCC	HT	$nb = 10$	955	$nb = 10$	3036
BCC	LT	$nv = 10$	2647	$nv = 9$	1208
FCC	HT	$nb = 10$	2575	$nb = 10$	5412
FCC	LT	$nv = 9$	7215	$nv = 7$	497

3. Series analysis

The series are analysed in the same way as in our previous paper (Hamer *et al* 1992). Firstly, we have calculated standard Dlog Padé approximants and confluent differential

Table 2. High-temperature series in λ for the ground-state energy per site E_0/N, the susceptibility χ, and the energy gap F. Coefficients of λ^n are listed.

n	E_0/N	χ	F
SC lattice			
0	-2	$\frac{1}{3}$	3
1	0	$\frac{4}{3}$	-6
2	$-1.000\,000\,000\,000$	$5.222\,222\,222\,222$	$-7.000\,000\,000\,000$
3	$-1.666\,666\,666\,667\times10^{-1}$	$2.022\,222\,222\,222\times10^{1}$	$-5.833\,333\,333\,333$
4	$-8.981\,481\,481\,481\times10^{-1}$	$7.943\,552\,812\,071\times10^{1}$	$-4.617\,592\,592\,593\times10^{1}$
5	$-8.389\,917\,695\,473\times10^{-1}$	$3.103\,366\,928\,314\times10^{2}$	$2.365\,226\,337\,449$
6	$-3.340\,577\,846\,365$	$1.223\,701\,032\,701\times10^{3}$	$-6.031\,975\,308\,642\times10^{2}$
7	$-5.638\,850\,784\,941$	$4.815\,699\,910\,857\times10^{3}$	$9.306\,210\,665\,612\times10^{2}$
8	$-2.031\,457\,327\,592\times10^{1}$	$1.905\,170\,031\,724\times10^{4}$	$-1.071\,616\,527\,727\times10^{4}$
9	$-4.573\,804\,931\,437\times10^{1}$	$7.533\,772\,271\,283\times10^{4}$	$3.151\,993\,522\,458\times10^{4}$
10	$-1.587\,276\,625\,348\times10^{2}$	$2.988\,695\,129\,945\times10^{5}$	$-2.311\,414\,620\,311\times10^{5}$
BCC lattice			
0	-2	$\frac{1}{3}$	3
1	0	$\frac{16}{9}$	-8
2	$-1.333\,333\,333\,333$	$9.333\,333\,333\,333$	$-1.200\,000\,000\,000\times10^{1}$
3	$-2.222\,222\,222\,222\times10^{-1}$	$4.869\,135\,802\,469\times10^{1}$	$-1.800\,000\,000\,000\times10^{1}$
4	$-2.876\,543\,209\,877$	$2.580\,475\,537\,266\times10^{2}$	$-1.512\,469\,135\,802\times10^{2}$
5	$-2.825\,102\,880\,658$	$1.361\,559\,967\,146\times10^{3}$	$-3.196\,159\,122\,085\times10^{1}$
6	$-1.946\,843\,087\,944\times10^{1}$	$7.254\,552\,553\,547\times10^{3}$	$-3.596\,040\,656\,912\times10^{3}$
7	$-3.751\,299\,767\,989\times10^{1}$	$3.857\,533\,398\,110\times10^{4}$	$6.806\,522\,608\,342\times10^{3}$
8	$-2.128\,585\,763\,959\times10^{2}$	$2.063\,374\,574\,071\times10^{5}$	$-1.179\,695\,462\,372\times10^{5}$
9	$-5.778\,013\,647\,783\times10^{2}$	$1.102\,935\,928\,829\times10^{6}$	$4.613\,535\,500\,834\times10^{5}$
10	$-3.008\,315\,976\,972\times10^{3}$	$5.917\,649\,543\,065\times10^{6}$	$-4.744\,191\,435\,498\times10^{6}$
FCC lattice			
0	-2	$\frac{1}{3}$	3
1	0	$\frac{8}{3}$	-12
2	$-2.000\,000\,000\,000$	$2.111\,111\,111\,111\times10^{1}$	$-2.600\,000\,000\,000\times10^{1}$
3	$-3.000\,000\,000\,000$	$1.680\,000\,000\,000\times10^{2}$	$-9.500\,000\,000\,000\times10^{1}$
4	$-9.759\,259\,259\,259$	$1.343\,645\,404\,664\times10^{3}$	$-5.225\,000\,000\,000\times10^{2}$
5	$-3.831\,584\,362\,140\times10^{1}$	$1.079\,220\,780\,623\times10^{4}$	$-2.943\,771\,604\,938\times10^{3}$
6	$-1.771\,601\,794\,696\times10^{2}$	$8.698\,374\,416\,855\times10^{4}$	$-1.894\,166\,706\,676\times10^{4}$
7	$-9.016\,458\,238\,073\times10^{2}$	$7.030\,865\,138\,995\times10^{5}$	$-1.226\,742\,463\,198\times10^{5}$
8	$-4.928\,367\,755\,668\times10^{3}$	$5.696\,701\,673\,531\times10^{6}$	$-8.451\,015\,776\,007\times10^{5}$
9	$-2.840\,995\,631\,321\times10^{4}$	$4.625\,170\,576\,728\times10^{7}$	$-5.863\,270\,819\,922\times10^{6}$
10	$-1.707\,282\,143\,449\times10^{5}$	$3.761\,831\,987\,155\times10^{8}$	$-3.513\,639\,754\,349\times10^{7}$

approximants (Guttmann 1989) to the series for the derivative of the ground-state energy per site, the magnetization, susceptibility, and mass gap, as for a model with a normal second-order phase transition. The results are exhibited in table 5. From this table, as in the case of (2+1)-dimensions, it can be seen that the apparent second-order critical points derived from the magnetization, susceptibility, and mass-gap series are in good agreement with one another in every case, so we assume henceforth that they are the same for each different quantity. However, the critical points derived from the HT and LT series, λ_c^H and λ_c^L, respectively, 'cross over' each other by a small but significant amount, which is several times bigger than our expected errors. If the transition were really second-order, the two results should agree. This provides the first signal that the system actually undergoes a first-order transition, located somewhere in between the two pseudo-critical points λ_c^H and λ_c^L.

Table 3. Low-temperature series in λ' for the ground-state energy per site E_0'/N, the spontaneous magnetization M_0', the susceptibility χ', and the symmetric energy gap F'^{S}. Coefficients of λ'^n are listed.

n	E_0'/N	M_0'	χ'	F'^{S}
SC lattice				
0	-6	1	0	18
1	0	0	0	-1
2	$-1.111\,111\,111\,111\times10^{-1}$	$-9.259\,259\,259\,259\times10^{-3}$	$1.543\,209\,876\,543\times10^{-3}$	$-2.444\,444\,444\,444\times10^{-1}$
3	$-6.172\,839\,506\,173\times10^{-3}$	$-1.028\,806\,584\,362\times10^{-3}$	$2.572\,016\,460\,905\times10^{-4}$	$-4.358\,024\,691\,358\times10^{-2}$
4	$-2.556\,428\,482\,354\times10^{-4}$	$-1.220\,680\,429\,435\times10^{-4}$	$6.170\,451\,925\,987\times10^{-5}$	$-6.092\,405\,536\,850\times10^{-4}$
5	$-4.191\,434\,232\,586\times10^{-5}$	$-2.768\,886\,856\,678\times10^{-5}$	$1.770\,986\,807\,567\times10^{-5}$	$5.089\,734\,796\,525\times10^{-4}$
6	$-6.011\,025\,192\,033\times10^{-6}$	$-4.747\,607\,446\,829\times10^{-6}$	$3.841\,457\,261\,053\times10^{-6}$	$-9.912\,953\,208\,087\times10^{-5}$
7	$-6.948\,480\,357\,121\times10^{-7}$	$-8.211\,481\,846\,745\times10^{-7}$	$8.834\,544\,897\,968\times10^{-7}$	$-5\,016\,967\,814\,166\times10^{-5}$
8	$-1.196\,782\,824\,050\times10^{-7}$	$-1.690\,780\,384\,120\times10^{-7}$	$2.139\,141\,521\,777\times10^{-7}$	$-1.002\,917\,757\,395\times10^{-5}$
9	$-2.141\,254\,688\,487\times10^{-8}$	$-3.403\,005\,832\,857\times10^{-8}$	$4.999\,414\,633\,801\times10^{-8}$	$1.108\,362\,181\,717\times10^{-6}$
10	$-3.687\,509\,073\,179\times10^{-9}$	$-6.921\,346\,442\,452\times10^{-9}$	$1.179\,976\,787\,143\times10^{-8}$	$4.780\,193\,020\,099\times10^{-7}$
11	$-6.778\,125\,003\,024\times10^{-10}$	$-1.445\,281\,092\,932\times10^{-9}$	$2.784\,060\,734\,643\times10^{-9}$	$-1.945\,229\,363\,945\times10^{-8}$
12	$-1.251\,673\,004\,394\times10^{-10}$	$-3.004\,751\,926\,492\times10^{-10}$	$6.504\,686\,032\,228\times10^{-10}$	$-4.571\,257\,127\,331\times10^{-8}$
13	$-2.357\,367\,070\,939\times10^{-11}$	$-6.343\,809\,181\,457\times10^{-11}$	$1.528\,491\,161\,854\times10^{-10}$	$-6.765\,939\,615\,858\times10^{-9}$
14	$-4.635\,916\,254\,394\times10^{-12}$	$-1.364\,258\,348\,655\times10^{-11}$	$3.605\,485\,935\,190\times10^{-11}$	$1.482\,429\,783\,084\times10^{-9}$
15	$-9.225\,229\,574\,984\times10^{-13}$	$-2.947\,845\,552\,935\times10^{-12}$	$8.494\,403\,226\,235\times10^{-12}$	$6.077\,104\,103\,456\times10^{-10}$
16	$-1.843\,786\,072\,533\times10^{-13}$	$-6.397\,133\,883\,497\times10^{-13}$	$2.000\,921\,892\,612\times10^{-12}$	$-2.721\,973\,067\,010\times10^{-11}$
17	$-3.725\,969\,289\,577\times10^{-14}$	$-1.395\,843\,195\,160\times10^{-13}$	$4.713\,078\,687\,905\times10^{-13}$	$-4.935\,736\,693\,247\times10^{-11}$
18	$-7.609\,606\,215\,014\times10^{-15}$	$-3\,060\,948\,051\,571\times10^{-14}$	$1.110\,412\,442\,686\times10^{-13}$	
19	$-1.570\,704\,085\,807\times10^{-15}$	$-6.748\,881\,949\,784\times10^{-15}$	$2.618\,288\,700\,630\times10^{-14}$	
20	$-3.271\,173\,741\,747\times10^{-16}$	$-1.494\,572\,839\,100\times10^{-15}$	$6.176\,147\,442\,054\times10^{-15}$	
21	$-6.853\,248\,480\,703\times10^{-17}$	$-3.320\,263\,557\,927\times10^{-16}$	$1.456\,922\,692\,516\times10^{-15}$	
BCC lattice				
0	-8	1	0	24
1	0	0	0	-1
2	$-8.333\,333\,333\,333\times10^{-2}$	$-5.208\,333\,333\,333\times10^{-3}$	$6.510\,416\,666\,667\times10^{-4}$	$-1.507\,936\,507\,937\times10^{-1}$
3	$-3.472\,222\,222\,222\times10^{-3}$	$-4.340\,277\,777\,778\times10^{-4}$	$8\,138\,020\,833\,333\times10^{-5}$	$-2.114\,827\,412\,446\times10^{-2}$
4	$-9.782\,848\,324\,515\times10^{-5}$	$-3.529\,715\,319\,770\times10^{-5}$	$1.331\,663\,123\,895\times10^{-5}$	$-4.346\,591\,494\,645\times10^{-4}$
5	$-1.119\,516\,093\,474\times10^{-5}$	$-5.751\,360\,150\,542\times10^{-6}$	$2.772\,702\,608\,863\times10^{-6}$	$4.178\,823\,183\,897\times10^{-5}$
6	$-1.222\,321\,004\,630\times10^{-6}$	$-7.283\,797\,024\,595\times10^{-7}$	$4.390\,198\,857\,270\times10^{-7}$	$-2.032\,601\,379\,581\times10^{-5}$
7	$-1.026\,091\,107\,415\times10^{-7}$	$-9.098\,477\,519\,633\times10^{-8}$	$7.280\,520\,513\,400\times10^{-8}$	$-5.735\,082\,941\,307\times10^{-6}$
8	$-1.289\,252\,768\,835\times10^{-8}$	$-1.368\,521\,685\,986\times10^{-8}$	$1.286\,685\,179\,205\times10^{-8}$	$-8.575\,020\,534\,183\times10^{-7}$
9	$-1.727\,550\,934\,237\times10^{-9}$	$-2.032\,814\,027\,219\times10^{-9}$	$2.204\,496\,244\,978\times10^{-9}$	$1.592\,510\,613\,274\times10^{-8}$
10	$-2.209\,920\,093\,330\times10^{-10}$	$-3.041\,228\,635\,574\times10^{-10}$	$3.811\,360\,802\,420\times10^{-10}$	$1.132\,210\,500\,806\times10^{-8}$
11	$-2\,993\,811\,666\,934\times10^{-11}$	$-4.667\,813\,357\,152\times10^{-11}$	$6.595\,267\,929\,160\times10^{-11}$	$-6.277\,793\,857\,060\times10^{-10}$
12	$-4.078\,772\,532\,507\times10^{-12}$	$-7.138\,925\,397\,155\times10^{-12}$	$1.130\,888\,729\,648\times10^{-11}$	$-7.385\,158\,640\,199\times10^{-10}$
13	$-5.661\,157\,507\,143\times10^{-13}$	$-1.107\,818\,692\,739\times10^{-12}$	$1.949\,704\,539\,693\times10^{-12}$	$-8.962\,012\,572\,575\times10^{-11}$
14	$-8.178\,362\,485\,030\times10^{-14}$	$-1.748\,889\,351\,242\times10^{-13}$	$3.372\,661\,671\,175\times10^{-13}$	$5.640\,421\,374\,971\times10^{-12}$
15	$-1.194\,572\,363\,559\times10^{-14}$	$-2.773\,109\,973\,200\times10^{-14}$	$5.826\,464\,647\,715\times10^{-14}$	$2.588\,496\,912\,292\times10^{-12}$
16	$-1.754\,214\,611\,880\times10^{-15}$	$-4.417\,818\,701\,387\times10^{-15}$	$1.006\,660\,631\,544\times10^{-14}$	$-8.677\,815\,036\,271\times10^{-14}$
17	$-2.606\,405\,330\,562\times10^{-16}$	$-7.078\,522\,796\,723\times10^{-16}$	$1.739\,499\,169\,217\times10^{-15}$	$-1.157\,685\,975\,097\times10^{-13}$
18	$-3.913\,469\,658\,937\times10^{-17}$	$-1.139\,856\,248\,161\times10^{-16}$	$3.006\,789\,181\,458\times10^{-16}$	
19	$-5.937\,191\,246\,550\times10^{-18}$	$-1.845\,429\,149\,667\times10^{-17}$	$5.201\,875\,312\,327\times10^{-17}$	
20	$-9.087\,021\,610\,971\times10^{-19}$	$-3.000\,913\,323\,807\times10^{-18}$	$9.003\,489\,058\,979\times10^{-18}$	
21	$-1.399\,166\,345\,334\times10^{-19}$	$-4.895\,644\,363\,149\times10^{-19}$	$1.558\,556\,739\,939\times10^{-18}$	

Next, we have used a first-order inhomogeneous differential approximant (Guttmann 1989) to extrapolate both the high- and low-temperature series to the transition point, starting from the high- and low-temperature limits, respectively.

Figure 1 show the results for the ground-state energy per site. It can be seen that the high- and low-temperature extrapolations cross each other at a distinct angle, which is again characteristic of a first-order transition. The transition point where the two lines cross is

Table 3. Continued.

n	E'_0/N	M'_0	χ'	F'^S
FCC lattice				
0	−12	1	0	36
1	0	0	0	−1
2	$-5.555\,555\,555\,556\times10^{-2}$	$-2.314\,814\,814\,815\times10^{-3}$	$1.929\,012\,345\,679\times10^{-4}$	$-8.282\,828\,282\,828\times10^{-2}$
3	$-1.543\,209\,876\,543\times10^{-3}$	$-1.286\,008\,230\,453\times10^{-4}$	$1.607\,510\,288\,066\times10^{-5}$	$-8.141\,006\,019\,794\times10^{-3}$
4	$-2.626\,235\,516\,735\times10^{-5}$	$-6.380\,834\,814\,231\times10^{-6}$	$1.599\,439\,036\,078\times10^{-6}$	$-2.538\,647\,992\,728\times10^{-4}$
5	$-1.840\,247\,467\,819\times10^{-6}$	$-6.609\,801\,510\,974\times10^{-7}$	$2.141\,947\,953\,736\times10^{-7}$	$-2.100\,808\,824\,929\times10^{-5}$
6	$-1.422\,170\,212\,807\times10^{-7}$	$-5.685\,389\,662\,316\times10^{-8}$	$2.273\,965\,448\,599\times10^{-8}$	$-2.684\,816\,122\,705\times10^{-6}$
7	$-8.585\,559\,477\,659\times10^{-9}$	$-4.864\,809\,102\,635\times10^{-9}$	$2.537\,202\,330\,097\times10^{-9}$	$-1.625\,890\,790\,776\times10^{-7}$
8	$-7.155\,787\,647\,254\times10^{-10}$	$-4.834\,471\,244\,440\times10^{-10}$	$2.956\,861\,967\,921\times10^{-10}$	$-1.961\,534\,388\,598\times10^{-8}$
9	$-6.045\,796\,454\,435\times10^{-11}$	$-4.645\,133\,168\,797\times10^{-11}$	$3.301\,732\,513\,878\times10^{-11}$	$-1.601\,681\,712\,471\times10^{-9}$
10	$-4\,960\,683\,287\,853\times10^{-12}$	$-4.523\,890\,287\,125\times10^{-12}$	$3.734\,126\,348\,431\times10^{-12}$	$-1.829\,770\,341\,440\times10^{-10}$
11	$-4\,455\,387\,247\,787\times10^{-13}$	$-4.581\,547\,740\,962\times10^{-13}$	$4.255\,855\,904\,068\times10^{-13}$	$-1.507\,626\,560\,856\times10^{-11}$
12	$-4.054\,811\,081\,451\times10^{-14}$	$-4\,636\,219\,335\,754\times10^{-14}$	$4.811\,926\,457\,938\times10^{-14}$	$-1.861\,399\,925\,108\times10^{-12}$
13	$-3.718\,146\,662\,083\times10^{-15}$	$-4.739\,792\,191\,524\times10^{-15}$	$5.459\,429\,241\,490\times10^{-15}$	$-1.566\,561\,703\,981\times10^{-13}$
14	$-3.516\,589\,112\,827\times10^{-16}$	$-4.912\,685\,789\,617\times10^{-16}$	$6.204\,930\,758\,576\times10^{-16}$	
15	$-3.364\,743\,646\,828\times10^{-17}$	$-5.115\,218\,358\,742\times10^{-17}$	$7.043\,584\,708\,835\times10^{-17}$	
16	$-3.252\,676\,903\,047\times10^{-18}$	$-5.361\,749\,527\,332\times10^{-18}$	$8.004\,406\,573\,027\times10^{-18}$	
17	$-3.189\,008\,286\,853\times10^{-19}$	$-5.657\,995\,418\,076\times10^{-19}$	$9.101\,883\,983\,774\times10^{-19}$	
18	$-3.154\,936\,332\,323\times10^{-20}$	$-5.997\,094\,989\,293\times10^{-20}$	$1.035\,049\,331\,350\times10^{-19}$	
19	$-3.147\,413\,798\,576\times10^{-21}$	$-6.386\,022\,364\,424\times10^{-21}$	$1.177\,689\,557\,883\times10^{-20}$	

Table 4. Low-temperature series in λ' for the the antisymmetric energy gap F'^A. Coefficients of λ'^n are listed for SC, BCC and FCC lattices.

n	SC	BCC	FCC
0	18	24	36
1	1	1	1
2	$-2.222\,222\,222\,222\times10^{-1}$	$-1.388\,888\,888\,889\times10^{-1}$	$-7.777\,777\,777\,778\times10^{-2}$
3	$-4.012\,345\,679\,012\times10^{-2}$	$-1.813\,271\,604\,938\times10^{-2}$	$-6.604\,938\,271\,605\times10^{-3}$
4	$-2.162\,052\,625\,016\times10^{-3}$	$-8.315\,833\,257\,963\times10^{-4}$	$-2.869\,177\,551\,142\times10^{-4}$
5	$-6.239\,521\,414\,419\times10^{-5}$	$-6.415\,565\,708\,583\times10^{-5}$	$-2.765\,258\,584\,095\times10^{-5}$
6	$-5.843\,750\,745\,313\times10^{-5}$	$-1.590\,500\,146\,691\times10^{-5}$	$-2.647\,079\,425\,129\times10^{-6}$
7	$-2.915\,056\,618\,858\times10^{-5}$	$-3.669\,510\,359\,450\times10^{-6}$	$-2.158\,856\,562\,623\times10^{-7}$
8	$-7.100\,136\,853\,245\times10^{-6}$	$-6.022\,304\,202\,888\times10^{-7}$	$-2.101\,101\,145\,780\times10^{-8}$
9	$-7.132\,993\,913\,832\times10^{-7}$	$-6.057\,897\,577\,185\times10^{-8}$	$-2.078\,770\,069\,957\times10^{-9}$
10	$3.683\,100\,118\,840\times10^{-8}$	$-4.578\,878\,965\,521\times10^{-9}$	$-2.007\,727\,365\,188\times10^{-10}$
11	$6.130\,499\,801\,574\times10^{-10}$	$-8.777\,724\,370\,899\times10^{-10}$	$-2.029\,289\,101\,115\times10^{-11}$
12	$-1.007\,235\,768\,774\times10^{-8}$	$-2.485\,091\,393\,533\times10^{-10}$	$-2.075\,072\,396\,612\times10^{-12}$
13	$-3.468\,909\,272\,944\times10^{-9}$	$-4.678\,438\,563\,202\times10^{-11}$	$-2.123\,157\,845\,438\times10^{-13}$
14	$-4.458\,181\,235\,969\times10^{-10}$	$-5.707\,898\,751\,330\times10^{-12}$	
15	$2.205\,994\,697\,882\times10^{-11}$	$-5.358\,262\,683\,666\times10^{-13}$	
16	$8.960\,752\,120\,726\times10^{-12}$	$-8.320\,342\,229\,591\times10^{-14}$	
17	$-3.619\,958\,517\,938\times10^{-12}$	$-2.179\,543\,431\,286\times10^{-14}$	

found to be

$$\begin{aligned}\lambda_c &= 0.2403(2) \quad \text{(SC lattice)}\\ \lambda_c &= 0.17655(20) \text{(BCC lattice)}\\ \lambda_c &= 0.1162(1) \quad \text{(FCC lattice)}.\end{aligned} \tag{3.1}$$

These lie neatly in between the pseudo-critical points λ_c^H and λ_c^L listed in table 5. The

Table 5. Estimates of singularity parameters for the pseudo second-order phase transitions, obtained by Dlog Padé approximants and confluent differential approximants to the series given in tables 2, 3 and 4.

	HT		LT	
Quantity	λ_c^H	Index	λ_c^L	Index
SC lattice				
M			0.237(2)	0.20(4)
χ	0.249(3)	−0.86(3)	0.2369(6)	−0.92(1)
F_S	0.250(4)	0.47(3)	0.236(2)	0.47(3)
F_A			0.237(1)	0.20(2)
BCC lattice				
M			0.172(3)	0.21(3)
χ	0.183(3)	−0.84(5)	0.173(1)	−0.95(5)
F_S	0.184(4)	0.48(5)	0.1730(6)	0.47(2)
F_A			0.172(1)	0.22(2)
FCC lattice				
M			0.115(3)	0.20(3)
χ	0.121(1)	−0.84(5)	0.114(1)	−0.91(5)
F_S	0.1207(8)	0.44(3)	0.1143(5)	0.44(2)
F_A			0.114(1)	0.20(3)

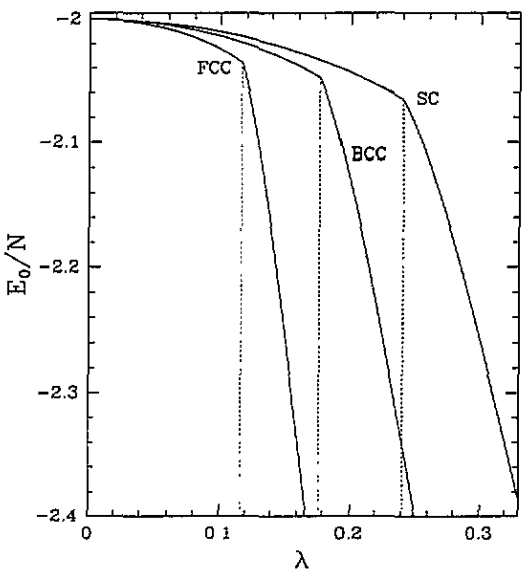

Figure 1. Graph of the ground state energy per site E_0/N against λ for the SC, BCC and FCC lattices. The broken vertical lines mark the expected phase transitions.

remaining functions, namely the magnetization, the susceptibility and the mass gap (and also the derivative of the low-temperature ground-state energy), vary rapidly near the transition point because of the nearby pseudo-critical point. It is useful therefore to 'smooth' each of these functions before making the extrapolations (Liu and Fisher 1989), by calculating approximants to the series for $(1-\lambda/\lambda_c^{(s)})^{-\nu} f(\lambda)$ rather than $f(\lambda)$ itself, where $\lambda_c^{(s)}$ and ν are the pseudo-critical point and critical index, respectively. The errors arise mainly from the uncertainties in the critical parameters λ_c, $\lambda_c^{(s)}$ and ν in each case.

The results are as follows.

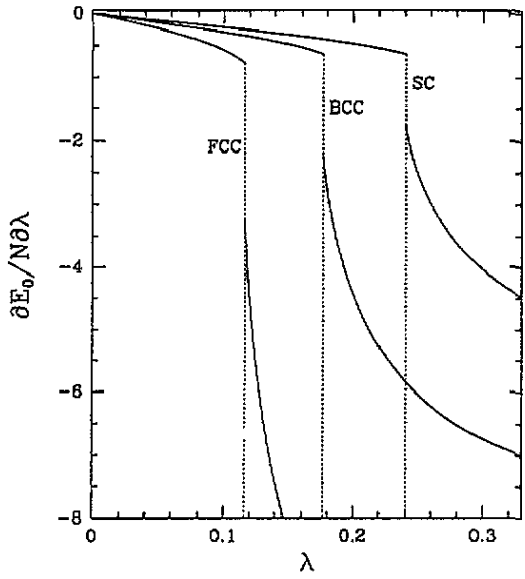

Figure 2. Graph of the derivative of the ground state energy per site, $(1/N)\partial E_0/\partial\lambda$ against λ for the SC, BCC and FCC lattices. The broken vertical lines mark the expected phase transitions.

Derivative of the ground-state energy. The derivative shows a substantial discontinuity at the transition point, as illustrated in figure 2

$$\frac{1}{N}\frac{dE_0}{d\lambda} = \begin{cases} -0.632(4) & \lambda \to \lambda_c- \\ -1.77(2) & \lambda \to \lambda_c+ \end{cases} \tag{3.2}$$

for the SC lattice, or

$$\frac{1}{N}\frac{dE_0}{d\lambda} = \begin{cases} -0.636(8) & \lambda \to \lambda_c- \\ -2.21(4) & \lambda \to \lambda_c+ \end{cases} \tag{3.3}$$

for the BCC lattice, or

$$\frac{1}{N}\frac{dE_0}{d\lambda} = \begin{cases} -0.781(3) & \lambda \to \lambda_c- \\ -3.22(2) & \lambda \to \lambda_c+ . \end{cases} \tag{3.4}$$

for the FCC lattice.

Thus we estimate the discontinuity or 'latent heat' as

$$L \equiv \frac{1}{N}\left(\left.\frac{\partial E_0}{\partial\lambda}\right|_{\lambda=\lambda_c-} - \left.\frac{\partial E_0}{\partial\lambda}\right|_{\lambda=\lambda_c+}\right) = \begin{cases} 1.14(2) & \text{(SC lattice)} \\ 1.57(4) & \text{(BCC lattice)} \\ 2.44(2) & \text{(FCC lattice)} . \end{cases} \tag{3.5}$$

Spontaneous magnetization. The spontaneous magnetization is shown in figure 3. At the transition point, the values are

$$M_0 = \begin{cases} 0.48(1) & \text{(SC lattice)} \\ 0.48(2) & \text{(BCC lattice)} \\ 0.48(1) & \text{(FCC lattice)} \end{cases} \tag{3.6}$$

i.e. about 48% of the maximum possible value for each lattice. The similarity between these values for all three lattices is very striking, and immediately suggests at least an approximate form of universality. To test this further, we plot the magnetization for all

three lattices against a 'reduced' coupling variable λ/λ_c in figure 4. It can be seen that the results for all three lattices, while not identical, certainly lie extremely close to one another, so that a 'law of corresponding states' seems to apply.

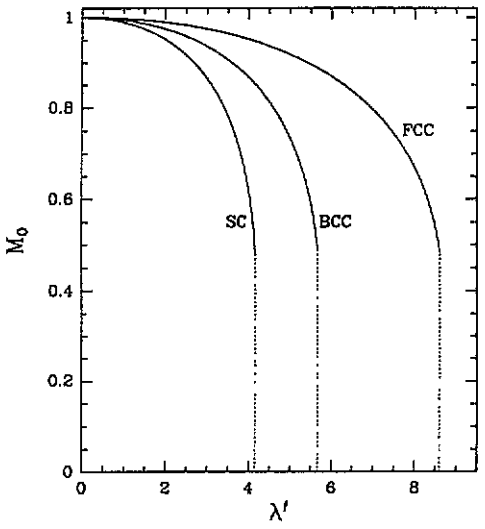

Figure 3. Graph of the spontaneous magnetization M_0 against λ' for the SC, BCC and FCC lattices.

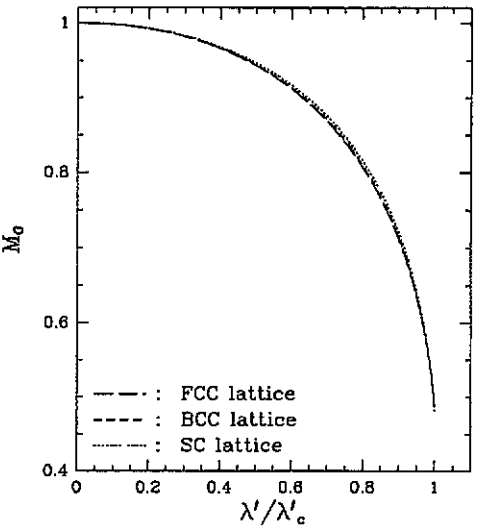

Figure 4. Graph of the spontaneous magnetization M_0 against the 'reduced' coupling λ'/λ'_c for the SC, BCC and FCC lattices.

Susceptibility. The data for the susceptibility† are displayed in a similar fashion in figures 5 and 6. Values at the transition point are

$$\chi = \begin{cases} 7.3(10) & \lambda \to \lambda_c- \\ 5.8(15) & \lambda \to \lambda_c+ \end{cases} \tag{3.7}$$

for the SC lattice, or

$$\chi = \begin{cases} 6.5(5) & \lambda \to \lambda_c- \\ 7(2) & \lambda \to \lambda_c+ \end{cases} \tag{3.8}$$

for the BCC lattice, or

† We take this opportunity of correcting an error in our previous paper (Hamer *et al* 1992), where a factor 4 was misplaced in the high-temperature series for the susceptibility χ for the square and triangular lattices, and a factor λ' was misplaced in the low-temperature series. After correcting these mistakes, the susceptibilities at the transition point are found to be

$$\chi = \begin{cases} 17(4) & \lambda \to \lambda_c- \\ 21(8) & \lambda \to \lambda_c+ \end{cases}$$

for the square lattice, or

$$\chi = \begin{cases} 29(4) & \lambda \to \lambda_c- \\ 16(4) & \lambda \to \lambda_c+ \end{cases}$$

for the triangular lattice.

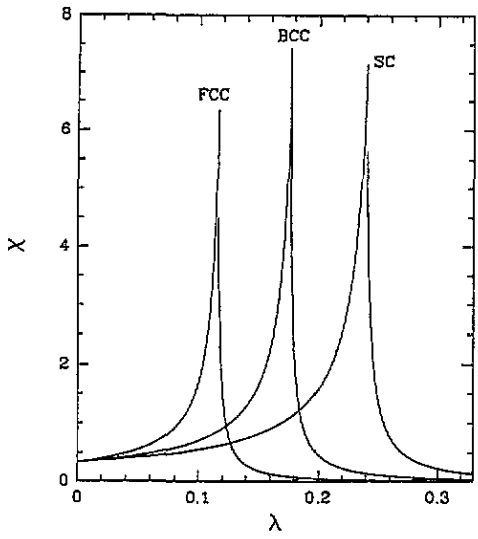

Figure 5. Graph of the susceptibility χ against λ for the SC, BCC and FCC lattices.

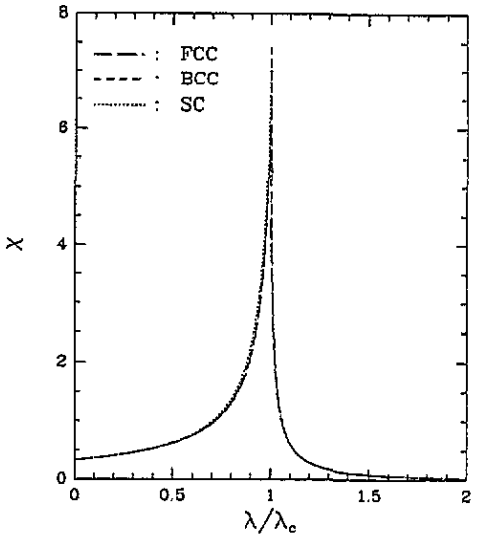

Figure 6. Graph of the susceptibility χ against the 'reduced' coupling λ/λ_c for the SC, BCC and FCC lattices.

$$\chi = \begin{cases} 6.3(4) & \lambda \to \lambda_c- \\ 5(2) & \lambda \to \lambda_c+ \end{cases} \tag{3.9}$$

for the FCC lattice.

Again it appears that the behaviour is very close to universal, and an approximate law of corresponding states is obeyed, as illustrated in figure 6.

Mass gaps. The symmetric and anti-symmetric mass gaps are displayed in figures 7 and 8. Values at the transition point are

$$F^S = \begin{cases} 0.59(5) & \lambda \to \lambda_c- \\ 0.8(2) & \lambda \to \lambda_c+ \end{cases}$$

$$F^A = \begin{cases} 0.59(5) & \lambda \to \lambda_c- \\ 2.40(15) & \lambda \to \lambda_c+ \end{cases} \tag{3.10}$$

for the SC lattice, and

$$F^S = \begin{cases} 0.63(4) & \lambda \to \lambda_c- \\ 0.82(8) & \lambda \to \lambda_c+ \end{cases}$$

$$F^A = \begin{cases} 0.63(4) & \lambda \to \lambda_c- \\ 2.62(12) & \lambda \to \lambda_c+ \end{cases} \tag{3.11}$$

for the BCC lattice, and

$$F^S = \begin{cases} 0.65(3) & \lambda \to \lambda_c- \\ 0.8(1) & \lambda \to \lambda_c+ \end{cases}$$

(3.12)

$$F^{A} = \begin{cases} 0.65(3) & \lambda \to \lambda_c - \\ 2.64(15) & \lambda \to \lambda_c + \end{cases}$$

for the FCC lattice.

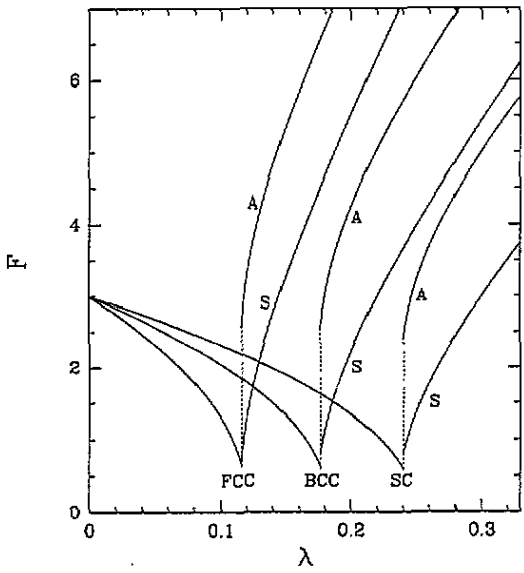

Figure 7. Graph of the symmetric and antisymmetric mass gap F^{S} and F^{A} against λ for the SC, BCC and FCC lattices.

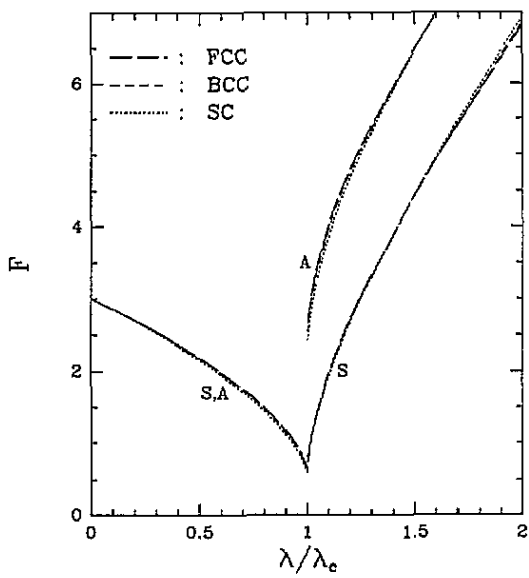

Figure 8. Graph of the symmetric and antisymmetric mass gap F^{S} and F^{A} against the 'reduced' coupling λ/λ_c for the SC, BCC and FCC lattices.

Once more, there is a striking similarity between these values for the different lattices, and a law of corresponding states is approximately obeyed (figure 8). The mass gap is small but finite at the transition point, as one would expect for a weak first-order transition; and our data indicate that the symmetric mass gap is either continuous, or has only a small discontinuity from the low-temperature to the high-temperature phase. The antisymmetric

mass gap, on the other hand, certainly seems to undergo a substantial discontinuity at the phase transition, as seen in figures 7 and 8.

Is it possible that the symmetric mass gap is really continuous, so that the singularity at the transition is a cusp rather than a finite discontinuity? This is precisely what happens in the Q-state Potts model in $(1+1)$ dimension for $Q > 4$, where a similar first-order transition occurs. Discussions of the finite-size behaviour of the low-lying energy eigenvalues for this system were given by Igloi and Solyom (1983) and Hamer (1983), for instance. On the other hand, the $(1+1)$D model possesses a self-duality property which enforces this continuity, and is not true of the $(3+1)$D model; and we certainly know of no general argument why continuity should occur. The values (3.10)–(3.12) nevertheless leave this as an intriguing conjecture. Similarly, the values (3.7)–(3.9) raise the possibility that the susceptibility might also be continuous, with a cusp singularity at the transition point, although we are aware of no good reason why this should be so.

Acknowledgment

This work forms part of a research project supported by a grant from the Australian Research Council.

References

Aharony A and Pytte E 1981 *Phys. Rev.* B **23** 362

Guttmann A J 1989 *Phase Transitions and Critical Phenomena* vol 13 ed C Domb and J Lebowitz (New York: Academic)

Hamer C J 1983 *J. Phys. A: Math. Gen.* **16** 3085.

Hamer C J, Oitmaa J and Zheng W H 1992 *J. Phys. A: Math. Gen.* **25** 1821

He H X, Hamer C J and Oitmaa J 1990 *J. Phys. A: Math. Gen.* **23** 1775

Igloi F and Solyom J 1983 *J. Phys. C: Solid State Phys.* **16** 2883

Liu A J and Fisher M E 1989 *Physica* **156A** 35

Nickel B G 1980 unpublished